Biosensors and Bioelectronics 128 (2019) 68–75

Contents lists available at ScienceDirect

Biosensors and Bioelectronics

journal homepage: www.elsevier.com/locate/bios

Silica bead-based microfluidic device with integrated photodiodes for the rapid capture and detection of rolling circle amplification products in the femtomolar range

Ruben R.G. Soares[a,c,1,2], Felix Neumann[b,1], Catarina R.F. Caneira[a,1], Narayanan Madaboosi[b,**,1], Sibel Ciftci[b], Iván Hernández-Neuta[b], Inês F. Pinto[a,c,2], Denis R. Santos[a,c], Virginia Chu[a], Aman Russom[e], João P. Conde[a,d,*], Mats Nilsson[b,**]

[a] Instituto de Engenharia de Sistemas e Computadores – Microsistemas e Nanotecnologias (INESC MN) and IN – Institute of Nanoscience and Nanotechnology, Lisbon, Portugal
[b] Science for Life Laboratory, Department of Biochemistry and Biophysics, Stockholm University, SE-171 65 Solna, Sweden
[c] IBB – Institute for Bioengineering and Biosciences, Instituto Superior Técnico, Universidade de Lisboa, Lisbon, Portugal
[d] Department of Bioengineering, Instituto Superior Técnico, Universidade de Lisboa, Lisbon, Portugal
[e] Science for Life Laboratory, Division of Proteomics and Nanobiotechnology, KTH Royal Institute of Technology, Stockholm, Sweden

ARTICLE INFO

Keywords:
Photodiodes
Rolling circle amplification
Infectious disease diagnostics
Microfluidics
Silica microbeads

ABSTRACT

The rapid and sensitive detection of specific nucleic acid sequences at the point-of-care (PoC) is becoming increasingly in demand for a variety of emergent biomedical applications ranging from infectious disease diagnostics to the screening of antimicrobial resistance. To meet such demand, considerable efforts have been invested towards the development of portable and integrated analytical devices combining microfluidics with miniaturized signal transducers.

Here, we demonstrate the combination of rolling circle amplification (RCA)-based nucleic acid amplification with an on-chip size-selective trapping of amplicons on silica beads (~8 nL capture chamber) coupled with a thin-film photodiode (200 × 200 μm area) fluorescence readout. Parameters such as the flow rate of the amplicon solution and trapping time were optimized as well as the photodiode measurement settings, providing minimum detection limits below 0.5 fM of targeted nucleic acids and requiring only 5 μL of pre-amplified sample. Finally, we evaluated the analytical performance of our approach by benchmarking it against a commercial instrument for RCA product (RCP) quantification and further investigated the effect of the number of RCA cycles and elongation times (ranging from 10 to 120 min). Moreover, we provide a demonstration of the application for diagnostic purposes by detecting RNA from influenza and Ebola viruses, thus highlighting its suitability for integrated PoC systems.

1. Introduction

Simple diagnostic devices are currently in high demand to address clinical needs at the Point-of-care (PoC), particularly concerning the screening of single-stranded RNA viruses such as Influenza and Ebola, having high mutation rates (Baseler et al., 2017; Taubenberger and Morens, 2008) and potential to cause devastating pandemics (Sanjuán et al., 2010; WHO, 2018a; WHO, 2018b). Fluorescence-based optical read-outs are the most common transduction method used for bioassays since they are characterized by high sensitivity and specificity (Yoo and Lee, 2016). However, fluorescence detection equipment is typically expensive, non-portable and requires trained personnel, thus being challenging to interface with miniaturized bioassays for field or PoC diagnostic applications (Sin et al., 2014; Soares et al., 2018; Wojciechowski et al., 2009). Semiconductor technology allows for true lab-on-a-chip (LoC) applications since optical systems can be

* Corresponding author at: Instituto de Engenharia de Sistemas e Computadores – Microsistemas e Nanotecnologias (INESC MN) and IN – Institute of Nanoscience and Nanotechnology, Lisbon, Portugal.
** Corresponding authors.
E-mail addresses: narayanan.srinivasan@scilifelab.se (N. Madaboosi), joao.conde@tecnico.ulisboa.pt (J.P. Conde), mats.nilsson@scilifelab.se (M. Nilsson).
[1] These authors contributed equally to this work.
[2] Present address: Science for Life Laboratory, Division of Proteomics and Nanobiotechnology, KTH Royal Institute of Technology, Stockholm, Sweden.

https://doi.org/10.1016/j.bios.2018.12.004
Received 4 October 2018; Received in revised form 26 November 2018; Accepted 3 December 2018
Available online 18 December 2018
0956-5663/

miniaturized and integrated along with the assay on-chip in a practical and economical fashion (Pinto et al., 2018a). In these systems, microfabricated photodiodes are ideal since they are portable, affordable, reusable and highly multiplexable for PoC devices (Obahiagbon et al., 2018; Soares et al., 2018). Thin-film hydrogenated amorphous silicon (*a*-Si:H) photodiodes, as integrated optical signal transducers, have demonstrated promising properties, such as low dark current, fabrication at low temperatures compatible with glass and plastic substrates, high quantum efficiency in the visible spectrum, as well as high sensitivity and a wide dynamic range (Pimentel et al., 2008; Pinto et al., 2018b).

Nucleic acid biosensors have revolutionized the field of diagnostics since they simplify traditional testing methods, both in terms of assay time and complexity, offering high specificity and sensitivity. In particular, those based on polymerase chain reaction (PCR) have shown outstanding performance for the diagnosis of genetic and infectious diseases in health care facilities (Kozel and Burnham-Marusich, 2017). However, PCR requires specialized instruments for power-intensive thermocycling, thus limiting their use at the PoC (Modak et al., 2016). In this context, isothermal amplification methods have been developed to overcome the need of thermocycling (Craw and Balachandran, 2012). In particular, rolling circle amplification (RCA) has proven to be a simple isothermal amplification technique that does not require extensive assay optimization and is typically robust against interferents (Conze et al., 2009; Fakruddin et al., 2013). Upon combining RCA with padlock probes (PLPs), a powerful molecular detection tool is created, finding numerous applications in the diagnostic field (Asalapuram et al., 2016; Mezger et al., 2014; Nilsson et al., 1994). RCA products (RCPs) comprise discrete molecules of ~1 μm in diameter, which by hybridizing fluorophore labeled complementary oligonucleotides, display a high local fluorescence intensity which can be imaged using standard low-magnification epifluorescence microscopy, thus making linear RCA-based amplification intrinsically digital, since each molecular recognition event generates one long ssDNA (~60 kb at ~1 kb/min (Dahl et al., 2004)). Different read-outs and biosensing strategies have been reported to detect RCPs, such as electrical (Guo et al., 2018; Russell et al., 2014), colorimetric (Asalapuram et al., 2016) or optomagnetic (Mezger et al., 2015). However, a simple and integrated RCP fluorescent read-out strategy has not been described and could be highly advantageous to simplify on-chip fluorescence signal transduction using linear RCA-based methods.

In this context, the use of silica microbeads to selectively isolate and concentrate nucleic acids is a practical, cost-effective and well-known procedure (Elphinstone et al., 2003), previously integrated in commercial DNA extraction kits (Ivanova et al., 2006) and miniaturized devices (Price et al., 2009). The interaction of DNA with silica at neutral pH occurs mostly by hydrophobic and ionic phosphate-silanol interactions (Shi et al., 2015), largely overcoming the negative charge repulsion between both molecules. These interactions are also known to be significantly promoted in the presence of high concentrations of chaotropic salts such as guanidinium chloride (GdnHCl) (Poeckh et al., 2008a). Moreover, the DNA capture efficiency is known to significantly decrease for short fragments, in the range of tens to a few hundred of base pairs, even at high salt concentrations, as it is the case of the non-specific free detection oligonucleotides (Liu et al., 2016). This combination of properties make silica-based extraction ideal for the selective capture and enrichment of RCPs. In this work, we develop and optimize the use of a silica bead-based microfluidic device integrated with a miniaturized thin-film photodiode for the enrichment and fluorescent detection of RCPs. For this, we characterize the microfluidic trapping of RCPs on silica beads and evaluate the sensitivity of the integrated *a*-Si:H photodiodes. We further demonstrate the diagnostic capabilities of our biosensor using RNA extracted from infected cell culture isolates of Influenza and Ebola viruses. Thus, this work points towards the development of simple bioassay schemes for microfluidic devices with integrated optical-to-electrical signal transduction to address the need for compact and portable biosensing platforms for biomedical applications.

2. Experimental methods

2.1. Rolling circle amplification (RCA), circle-to-circle amplification (C2CA) and quantification of RCA products (RCPs)

Details on viral isolates and reverse transcription can be found in the data supplement (Suppl. Note 1 and 2). Oligonucleotide sequences are summarized in Table S1. Padlock probe (PLP) ligation, RCA and C2CA procedures are described in detail in the data supplement (Suppl. Note 3 and 4). Briefly, after PLP ligation, RCA was performed in Φ29 DNA polymerase buffer containing 125 μM dNTPs, 0.2 μg/μL BSA and 400 mU/μL Φ29 DNA polymerase (Monserate Biotechnology Group, San Diego, USA) at 37 °C for 10–120 min followed by inactivation at 65 °C for 2 min. To perform C2CA, biotinylated cDNA with ligated PLPs was first captured on streptavidin-coated DynabeadsTM MyOneTM T1 (Life Technologies, Oslo, Norway). The beads were resuspended in 20 μL of amplification mixture (0.2 μg/μL BSA, 125 μM dNTPs and 200 mU/μL Φ29 DNA polymerase in Ampligase buffer) and incubated for 20 min at 37 °C, followed by 2 min enzyme inactivation at 65 °C. The second amplification mixture after monomerization contained 0.2 μg/μL BSA, 0.68 mM ATP, 14 mU/μL T4 DNA ligase, 125 μM dNTPs and 200 mU/μL Φ29 DNA polymerase in 10 μL Ampligase buffer. Amplification was performed for 60 min at 37 °C, followed by heat inactivation at 65 °C for 2 min. Experimental assay steps of C2CA are illustrated in Fig. 1-A. For quantification, RCPs were labeled by adding 30 μL hybridization buffer (1.4 M NaCl, 0.01% TWEEN® 20, 20 mM of Tris-HCl, pH 8 and EDTA) containing 5 nM of the respective detection oligonucleotide (Table S1) for 2 min at 75 °C and 20 min at 55 °C. RCPs from RCA and C2CA were quantified by amplified single-molecule detection (ASMD) using the dedicated instrument Aquila 400 from Q-linea (Uppsala, Sweden). The measurement average of technical duplicates was obtained, and the standard deviation was calculated.

2.2. Fabrication of microfluidic devices and liquid handling

The microfluidic devices were fabricated using standard polydimethylsiloxane (PDMS) mold replication techniques as previously described in detail (Pinto et al., 2017). Briefly, the Al hard masks were fabricated on glass substrates using direct write lithography (Heidelberg DWLII, Heidelberg Instruments Mikrotechnik, Germany) followed by wet Al etching (TechniEtch Al80 Aluminum etchant, Microchemicals, Germany). Two masks were used to define two different heights in an SU-8 negative photoresist mold, namely 20 and 100 μm using SU-8 2015 and 50 formulations, respectively (Microchem, Westborough, MA, USA). Each layer was spin coated to the final desired height and exposed through the respective hard mask to a UV light source (UV 400 W curing hand lamp from UV Light Technology Limited, UK). The SU-8 mold was then used to replicate several PDMS devices using a Sylgard 184 two-component kit from DOWSIL (Ellsworth Adhesives Iberica) at a 1:10 curing agent: pre-polymer ratio followed by a 90 min baking step at 70 °C. After baking, the PDMS structures were peeled off the mold, access holes were punched and the structures were sealed against microscope cover slips with an average thickness of 100 μm. An irreversible sealing against glass was performed after an oxygen plasma treatment for 60 s at a pressure of 850 mTorr and 11 W RF power (Expanded Plasma Cleaner, Harrick Plasma, Ithaca, NY, USA). Polyethylene tubing (BTPE-90), metallic adapters (SC 20/15) and 20 ga blunt syringe tips purchased from Instech Laboratories were used to connect the microfluidic device with a syringe pump (NE-4000, New Era Pump Systems Inc., Farmingdale, NY, USA).

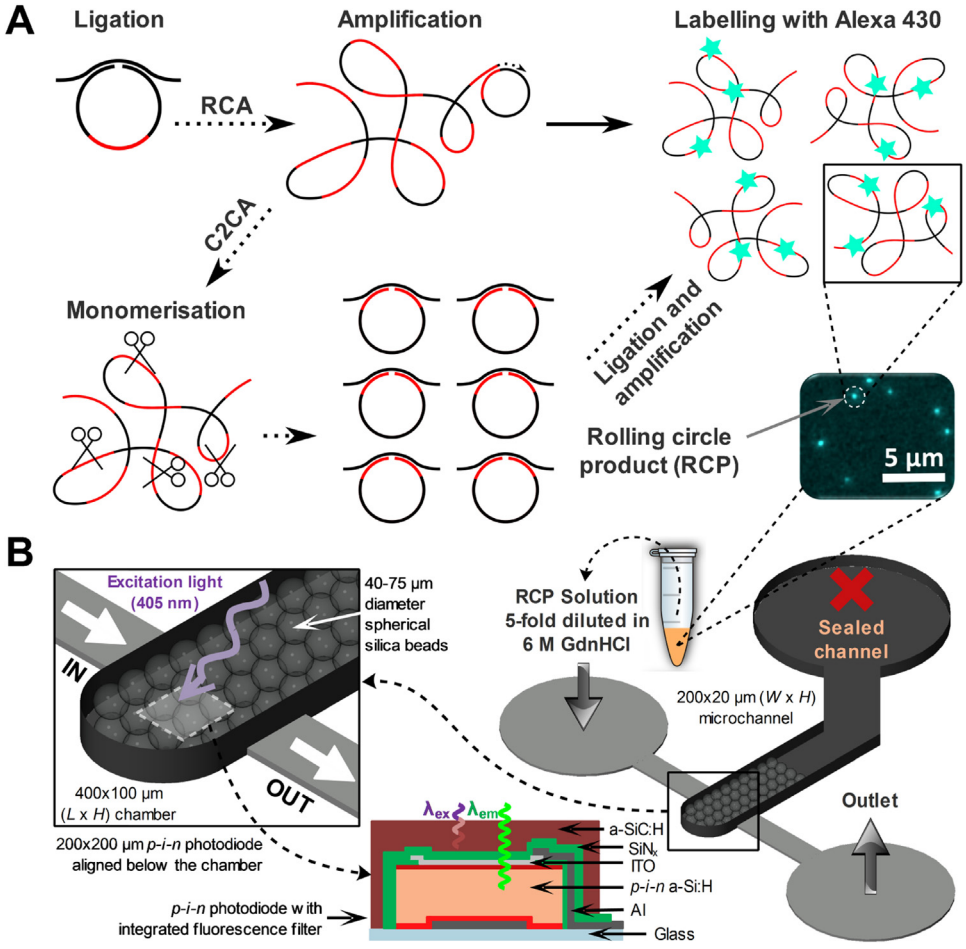

Fig. 1. Schematics of the off-chip target detection and amplification, followed by on-chip RCA product (RCP) capture and fluorescence signal transduction. A- Off-chip padlock probe (PLP)-based detection followed by rolling circle amplification (RCA) or circle-to-circle amplification (C2CA). The labelling of the RCPs is performed by hybridization using an excess concentration of detection oligonucleotides labeled with Alexa 430. B- On-chip RCP capture on silica beads after dilution in a chaotropic salt (guanidinium chloride) solution. The capture of the RCPs is continuously monitored by an a-Si:H photodiode aligned below the bead microcolumn. An a-SiC:H absorption filter is deposited on top of the photodiode to selectively block the excitation light (λ_{ex} = 405 nm) emitted by a laser diode, while being semi-transparent to the emission light (λ_{em} = 540 nm).

2.3. Packing of silica beads and capture of RCPs in the microfluidic device and fluorescence measurements using fluorescence microscopy

A suspension of mesoporous spherical silica beads (dried flash silica with 40–75 µm diameter and ~7 nm pores, purchased from Sigma-Aldrich) was first prepared in a solution of 20% (w/w) polyethylene glycol 8000 in water. After first pre-filling the device with water, the bead suspension was flowed into the 100 µm tall chamber at 10 µL/min by exerting a negative pressure at one of the outlets. The inlet of the 100 µm tall chamber was then sealed with a 20 ga metallic plug and the PEG solution was washed with water through the 20 µm tall channel. The RCP solution obtained in Sections 2.1 and 2.2 was then diluted 5-fold in an aqueous solution of 6 M guanidinium hydrochloride (≥99%, Sigma-Aldrich) and flowed through the 20 µm tall channel at flow-rates ranging from 1.25 to 50 µL/min. The trapping of RCPs was first monitored with fluorescence microscopy using a Leica DMLM microscope equipped with a DFC300FX digital camera and a 100 W mercury short-arc lamp coupled with a I3 filter cube. The illumination was performed discontinuously to periodically acquire images using an exposure time of 1 s. The quantitative analysis of the fluorescence signal was performed *via* grayscale measurements using the software ImageJ (National Institutes of Health, Bethesda, MA, USA). All solutions were prepared using type I water obtained from a Milli-Q system from Merck.

2.4. Fabrication of a-Si:H photodiodes

The thin-film *p-i-n* a-Si:H photodiodes were fabricated as described in detail elsewhere (Santos et al., 2017). In this work, an extra 1.8 µm thick layer of amorphous silicon carbide (a-SiC:H) was deposited by radio frequency plasma enhanced chemical vapor deposition (rf-PECVD) on top of the passivated sensors, followed by patterning by lift-off, functioning as an absorption filter to block the excitation light (λ_{ex} = 405 nm), while being semi-transparent to the emission light of the Alexa 430 fluorophore (λ_{max} = 540 nm). The photodiode dies were then diced and wire-bonded to custom-designed printed circuit boards (PCBs). The performance and spectral properties of this filter have also been described in detail elsewhere (Soares et al., 2018).

2.5. Instrumentation for photocurrent acquisition

The photodiode current at 0 V bias was measured using a Keithley 237 picoammeter connected to the PCB *via* coaxial and triaxial connections to minimize noise. The current measurements were acquired through GPIB and continuously processed and stored using a graphical user interface (GUI) programmed in Python and PyQT4. To perform the fluorescence measurements, the microfluidic device was first manually aligned directly on top of the photodiode and the 405 nm laser excitation light (photon flux (ϕ) = 1.04×10^{17} cm^{-2} s^{-1}), passing through the appropriate neutral density (ND) filter, was then aligned and focused on top of the bead-packed chamber to a final focal diameter of ~1 mm.

3. Results and discussion

3.1. Design of microfluidic device for RCP capture on silica microbeads

The main goal of this work was to develop a microfluidic device to perform the rapid quantification of RCPs resulting from the bioassay described in the schematics in Fig. 1-A. The microfluidic device integrating RCP capture, enrichment and fluorescence signal transduction

is schematized in Fig. 1-B. To perform the analysis, the RCP solution in hybridization buffer was first diluted 5-fold in 6 M GndHCl and then flowed through the silica bead-packed chamber. Upon illumination with a 405 nm laser light, the filtered photodiode aligned ~100 μm below the chamber allows the continuous and non-contact monitoring of Alexa 430-derived fluorescence emission, which is proportional to the number of captured RCPs on the silica beads. Considering the low bead volumes (few hundreds of nL) and mass of structural material (~1 g) required per PDMS device, these were designed to be disposable after a single measurement, *i.e.* no regeneration protocol was required to desorb the RCPs from the silica beads. Furthermore, considering that bare silica beads are used to perform direct RCP capture, the PDMS device containing packed beads can be stored for several years. Upon introduction of GdnHCl to the RCP solution, the hydrophobic and ionic phosphate-silanol interactions are significantly promoted (Poeckh et al., 2008b; Shi et al., 2015). In addition, the selectivity of silica towards long oligonucleotide molecules is ideal to minimize the background signal from the free detection oligonucleotides (25 bp).

3.2. Fluorescence microscopy imaging and flow-rate optimization

The capture of RCPs on the silica bead chamber was first monitored using fluorescence microscopy (Fig. 2-A). After flowing an RCP solution at 2.5 μL/min for 9 min through the chamber, a significant fluorescence signal could be measured. Interestingly, it was observed that the signal was highly heterogeneous and arranged as entangled and elongated filaments rather than individual dots, as previously observed in microfluidic assays where the RCPs are generated on the bead surface (Sato et al., 2010) or enriched on membranes (Kühnemund et al., 2017). These entangled filaments, hypothesized to be stretched RCPs, are dragged along the channel in the direction of the liquid flow, highlighting potential shear stress-derived effects, something similar to what has been reported for gold nanowire formation (Guo et al., 2018; Russell et al., 2014). Therefore, it was critical to subsequently evaluate the effect of flow-rate on RCP capture to achieve a balance between (i) RCP capture efficiency per flowed volume and (ii) RCP capture kinetics, thus maximizing signal output and minimizing assay time and reagent expenditure. On the other hand, flowing hybridization buffer containing free detection oligonucleotides (5 nM) did not provide a measurable increase in fluorescence above the background after 10 min.

The results obtained for the flow-rate optimization are shown in Fig. 2-B. We observed that the fluorescence intensity and slope (m) measured after flowing a fixed volume of solution are inversely proportional to the flow-rate down to 2.5 μL/min. A decrease in flow-rate down to 1.25 μL/min did not provide an increase in capture efficiency, resulting in a fluorescence intensity of 32.5 AU after flowing 50 μL of solution at t = 20 min, resulting in a two-fold increased detection time compared to using 2.5 μL/min. When evaluating the capture kinetics, the flow-rates of 2.5, 5 and 10 μL/min provided approximately the same signal intensity after the same amount of time, despite the two- and fourfold higher reagent expenditure using 5 and 10 μL/min. This trend implies that above 2.5 μL/min, the capture is already in reaction-limited conditions. On the other hand, the low signals measured above 10 μL/min indicate that a combination of high shear rates and/or low-residence times may be hindering the interaction of silica with the DNA molecules. Overall, a flow-rate of 2.5 μL/min provided an optimum balance between assay time and reagent consumption.

3.3. Monitoring conditions of RCP capture using a-Si:H photodiodes

To perform the continuous monitoring of RCP capture on the silica beads it was first necessary to optimize the illumination frequency and intensity of the excitation light, in order to minimize photobleaching without a significant compromise in temporal resolution (Fig. 3). By continuously illuminating the chamber with an incident photon flux (ϕ) of 3.1×10^{15} cm^{-2} s^{-1}, corresponding to an ND 1.5 filter (Fig. 3-A), it was observed that while the capture of RCPs could be effectively monitored above the laser excitation baseline (*i.e.* residual direct and scattered excitation light leaking through the a-SiC:H absorption filter), a pronounced photobleaching effect could be observed after stopping the liquid flow, having a very significant absolute rate of ~33% relative to the signal increase (*i.e.* $m_{signal} = 2.4 \times 10^{-15}$ A s^{-1} and $m_{bleach} = -8.0 \times 10^{-16}$ A s^{-1}). To minimize photobleaching effects, the excitation was performed discontinuously by turning ON the laser every minute for approximately 7.5 s (Fig. 3-B). This data is then normalized against the excitation baseline (henceforth referred to as specific photocurrent) and plotted over time as shown in Fig. 3-C. Comparing continuous and discontinuous illumination, the specific current after 10 min was observed to be 37.6% higher using the latter mode. Finally, the intensity of incident light was increased to $\phi = 1 \times 10^{16}$ cm^{-2} s^{-1} (ND 1.0) and $\phi = 3.1 \times 10^{16}$ cm^{-2} s^{-1} (ND 0.5) to optimize the emission output of the fluorophore. The results are shown in Fig. 3-D. It is possible to conclude that while the ND 1.0 provided a > 2-fold increase in fluorescence emission, a further increase in excitation photon flux (ND 0.5) did not provide an increased sensitivity, probably due to simultaneous increase in photobleaching effects, which become significant also in the discontinuous mode of excitation. Thus, the ND 1.0 was selected for the subsequent calibration curves at different concentrations of target genetic material.

3.4. Detection of Influenza A RNA and benchmarking against a commercial RCP counter

Using the optimized conditions for the read-out microfluidic device,

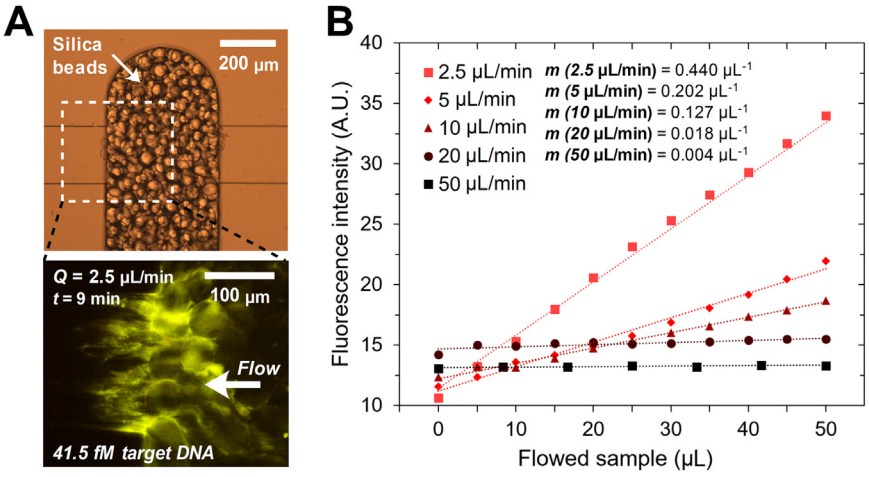

Fig. 2. A- Bright field (top) and fluorescence (bottom) microscopy imaging of the silica bead microcolumn and captured RCPs and B- flow-rate optimization. The fluorescence intensity values correspond to the grayscale values measured using an ROI of constant area positioned at the region of RCP concentration. A constant volume of 50 μL and concentration of 41.5 fM target influenza RNA, amplified using C2CA, was used for all experiments.

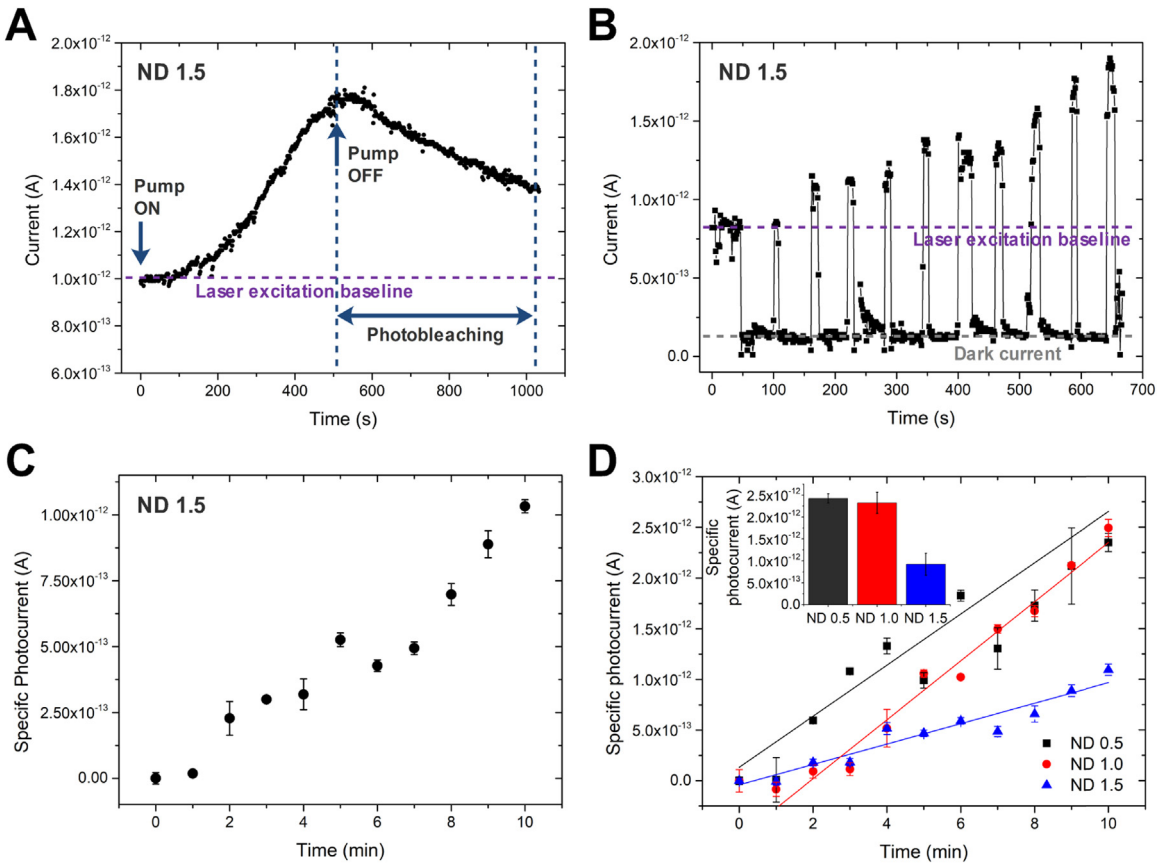

Fig. 3. Monitoring of RCP capture on the microfluidic device using the integrated photodiode (current values acquired at 1.25 s intervals). The 405 nm laser light used to excite the fluorophores was passed through different neutral density filters ranging from ND 1.5 to ND 0.5 as indicated in each plot, resulting in photon fluxes (ϕ) of ~3.1 × 10^{15} cm^{-2} s^{-1} up to 3.1 × 10^{16} cm^{-2} s^{-1}. A constant concentration of 41.5 fM target Influenza RNA, amplified using C2CA, was used for all experiments, flowed at 2.5 µL/min. A- Raw current measured for the continuous excitation of the silica microcolumn before and after stopping the flow of solution. B- Raw current measured for the discontinuous excitation of the bead microcolumn at 60 s intervals for an average pulse duration of 7.5 s. C- Average specific photocurrent measured over time for the data shown in plot B, calculated by subtracting the laser excitation baseline to all data acquired with the laser turned ON. The error bars correspond to ± SD of n ranging from 3 to 5 continuous points. D- Optimization of the ND filter used to perform the discontinuous excitation of the bead microcolumn. Error bars correspond to ± SD of n ranging from 3 to 5 continuous points. The inset plot shows the average specific photocurrent (± SD, n = 2) measured after 10 min for two independent experiments using each ND filter.

we tested its analytical performance by adapting a C2CA assay for the detection of Influenza A (Neumann et al., 2018). Serial dilutions of ssRNA from viral isolates were processed by reverse-transcription and C2CA (Fig. 1-A), and resulting RCPs were measured in parallel by our microfluidic read-out device and a commercial RCP counter. For each resulting RCP solutions, the specific photocurrent was monitored over time for 10 min, requiring a total sample volume of 5 µL (*i.e.* 25 µL of solution 5-fold diluted in GndHCl). The results are shown in Fig. 4-A. The RCP capture kinetics between 0 and 10 min could be fit to a linear regression. The data shows that the slope significantly increases above the baseline (*i.e.* sample "zero", without target genetic material) for increasing initial target concentrations and, despite the non-specific adsorption of free detection oligos being previously undetectable using the fluorescence microscopy setup (Section 3.2), here the sample "zero" also provides a measurable increase of 2.2 × 10^{-13} ± 1.9 × 10^{-14} A (t = 10 min) above the laser illumination background. The measured slopes were then plotted against the initial ssRNA concentration (Fig. 4-B) and the limit of detection (L_D), here defined as the target concentration which provides a signal equal to 3.29 times the standard deviation of the background (*i.e.* concentration of 0.28 fM which is not significantly different from the zero), was calculated as 0.46 ± 0.02 fM with a dynamic range of more than 2.7 orders of magnitude.

We obtained a high correlation between our microfluidic device and the commercial RCP counter (R^2 = 0.995) (Fig. 4-D), and by comparing practical features of both systems, the portability and low sample volumes (5 µL against 25 µL on the commercial system) intrinsic to our read-out are advantageous. Furthermore, depending on the sensitivity requirements, the analysis time and reagent volumes can be further reduced considering that significant signals above the laser excitation baseline could be measured in less than 2 min for target concentrations in the range of tens of femtomolar.

3.5. Optimization of amplification time with Ebola RNA extracts

Since the microfluidic-based readout was demonstrated to be able to detect RCPs in a short amount of time at initial target concentrations in the fM-range, we investigated the number of RCA cycles and elongation time required to generate a detectable fluorescence signal. For this, we compared first the photodiode response when performing RCA and C2CA on Ebola vRNA extracts. Fig. 5-A shows that both conditions result in a detectable fluorescence signal after only a few minutes of microfluidic trapping, thus demonstrating the suitability of both assays with the developed read-out. However, in this particular assay setup, RCA comes with the advantage of fewer assay steps (3 *vs.* 7 steps) when compared to C2CA, which facilitates eventual integration with the reported miniaturized device towards PoC applications.

Moreover, in order to optimize the total assay time, we further investigated the sensor response for increasing times of RCA. As shown in Fig. 5-B, a linear correlation (R^2 = 0.99) was obtained between elongation time and the measured slope. From the obtained linear

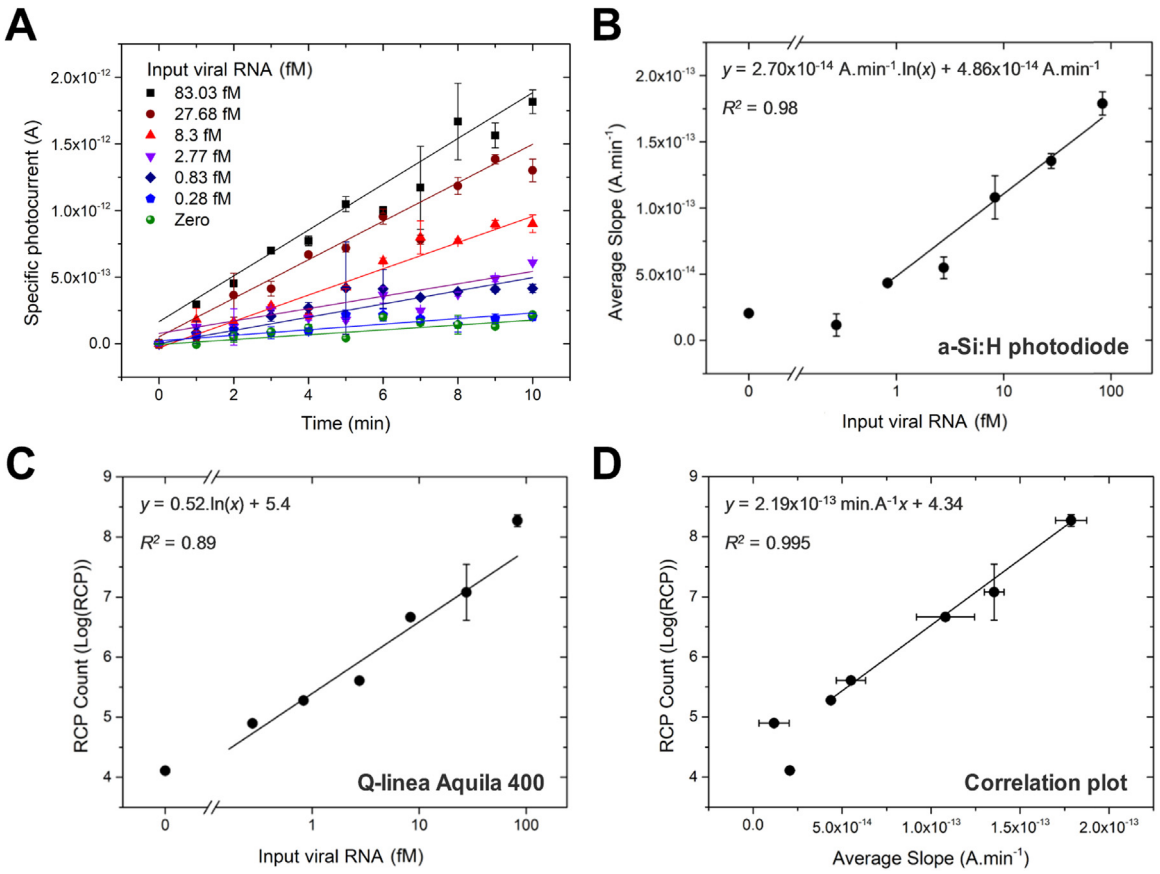

Fig. 4. Calibration curve for increasing target RNA concentrations and correlation with a commercial RCP counter (Q-linea Aquila 400). A- Specific photocurrent measured over time for increasing concentrations of Influenza RNA. The zero corresponds to a sample without target RNA, establishing the baseline for non-specific amplification and residual capture of free detection oligonucleotides. Error bars correspond to ± SD of n ranging from 3 to 5 continuous points. B- Average current slope measured between 0 and 10 min at increasing target RNA concentrations. Error bars correspond to ± SD of two independent measurements for each point. C- RCP counts for each viral RNA concentration measured using the Q-linea Aquila 400 instrument. D- Correlation between the RCP counts and the average current slope measured using the miniaturized device.

regression, the minimum amplification time necessary to provide a significant signal (3.29σ) above the background was calculated as 41.5 min. The linearity of generated signal was maintained throughout all elongation times proving the suitability of our trapping method for a wide-range of RCP sizes, estimated to range between 10,000 and 120,000 bp (Dahl et al., 2004), without a simultaneous loss of capture efficiency.

4. Conclusions

In conclusion, we have presented a novel and integrated read-out strategy for RCA-based assays in a microfluidic format by combining size-selective trapping on silica beads with miniaturized *p-i-n* a-Si:H photodiodes. Our device provided an effective, portable and affordable alternative over commercially available instruments for RCP detection with a wide dynamic range, resorting to sample volumes below 5 μL and achieving total assay sensitivities in the low femtomolar range (L_D < 0.5 fM). These figures of merit demonstrate comparable or superior sensitivities to recently reported paper-based diagnostic devices using reverse transcription loop-mediated isothermal amplification (RT-LAMP) for viral detection, combined with a dramatic decrease in sample requirements (5–10-fold) and automated signal transduction (Kaarj et al., 2018; Rodriguez et al., 2015). On the other hand, while superior sensitivities (~10-fold) were previously reported using fully integrated lab-on-disk devices coupled with RT-PCR amplification (Stumpf et al., 2016), significantly higher sample volumes (200 μL) were required.

Immediate future perspectives include the full integration of the RCA assay with the reported read-out, thereby bringing our approach closer to the PoC by avoiding the lengthy and laborious off-chip amplification procedures. Furthermore, since the use of PLPs offers high multiplex capability, the assay can be extended for the detection of several pathogens (Kühnemund et al., 2017) and implemented in a multiplexed format for a broader selection of targets, including antimicrobial resistance markers.

Acknowledgements

Influenza RNA extracts were kindly provided by Prof. Jan Albert, KI, Sweden, in the scope of SSF project FLU-ID. Ebola samples were kindly provided by Dr. Ali Mirazimi at the Public Health Agency of Sweden (FoHM) in the scope of IMI project, EbolaMoDRAD. BSL-4 facilities were from FoHM, Sweden. F. Neumann acknowledges the European Union's Horizon 2020 research and innovation program “New Diagnostics for Infectious Diseases” (ND4ID) [grant number 675412]. A. Russom acknowledges the Innovative Medicines Initiative 2 Joint Undertaking [grant agreement No 722208]. This Joint Undertaking, project iConsensus, receives support from the European Union's Horizon 2020 research and innovation programme and EFPIA Partners Sanofi, GSK, Bayer, Rentschler, UCB, Synthon and Pfizer. M. Nilsson acknowledges the Swedish Research Council. The authors also thank the Fundação para a Ciência e a Tecnologia (FCT) for funding through doctoral grants to R.R.G. Soares (SFRH/BD/97354/2013), C.R.F. Caneira (PD/BD/135274/2017), D.R. Santos (SFRH/BD/95079/2013)

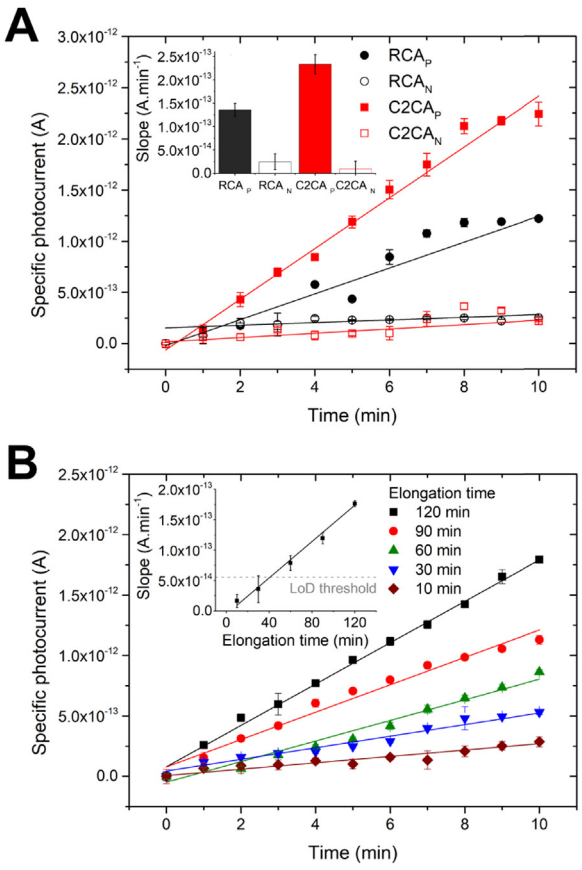

Fig. 5. Detection of Ebola vRNA using RCA and the miniaturized read-out device. A- Detection of resulting RCPs after one (RCA) or two (C2CA) cycles of amplification for positive (P) (14.3 ng μL^{-1} of viral RNA) or negative (N) (type I water only) samples. The inset plot shows the slope for technical replicates. B- Detection of RCPs generated using increasing RCA times. The inset plot shows the slope measured in duplicate for the same sample. The measurements shown in B were performed using synthetic DNA templates.

and I.F. Pinto (SFRH/BD/96442/2013), the research project OptLoc (PTDC/BBB-NAN/5927/2014) and through plurianual financing through the Institute of Nanoscience and Nanotechnology (UID/NAN/50024/2013).

Appendix A. Supporting information

Supplementary data associated with this article can be found in the online version at https://doi.org/10.1016/j.bios.2018.12.004.

References

Asalapuram, P.R., Engström, A., Liu, J., Herthnek, D., Nilsson, M., 2016. Proficient detection of multidrug-resistant mycobacterium tuberculosis by padlock probes and lateral flow nucleic acid biosensors. Anal. Chem. https://doi.org/10.1021/acs.analchem.5b04312.

Baseler, L., Chertow, D.S., Johnson, K.M., Feldmann, H., Morens, D.M., 2017. The pathogenesis of Ebola virus disease. Annu. Rev. Pathol. Mech. Dis. 12, 387–418. https://doi.org/10.1146/annurev-pathol-052016-100506.

Conze, T., Shetye, A., Tanaka, Y., Gu, J., Larsson, C., Göransson, J., Tavoosidana, G., Söderberg, O., Nilsson, M., Landegren, U., 2009. Analysis of genes, transcripts, and proteins via DNA ligation. Annu. Rev. Anal. Chem. 2, 215–239. https://doi.org/10.1146/annurev-anchem-060908-155239.

Craw, P., Balachandran, W., 2012. Isothermal nucleic acid amplification technologies for point-of-care diagnostics: a critical review. Lab Chip 12, 2469. https://doi.org/10.1039/c2lc40100b.

Dahl, F., Banér, J., Gullberg, M., Mendel-Hartvig, M., Landegren, U., Nilsson, M., 2004. Circle-to-circle amplification for precise and sensitive DNA analysis. Proc. Natl. Acad. Sci. USA 101, 4548–4553. https://doi.org/10.1073/pnas.0400834101.

Elphinstone, M.S., Hinten, G.N., Anderson, M.J., Nock, C.J., 2003. An inexpensive and high-throughput procedure to extract and purify total genomic DNA for population studies. Mol. Ecol. Notes 3, 317–320. https://doi.org/10.1046/j.1471-8286.2003.00397.x.

Fakruddin, M., Mannan, K.S., Bin, Chowdhury, A., Mazumdar, R.M., Hossain, M.N., Islam, S., Chowdhury, M.A., 2013. Nucleic acid amplification: alternative methods of polymerase chain reaction. J. Pharm. Bioallied Sci. 5, 245–252. https://doi.org/10.4103/0975-7406.120066.

Guo, M., Hernández-Neuta, I., Madaboosi, N., Nilsson, M., van der Wijngaart, W., 2018. Efficient DNA-assisted synthesis of trans-membrane gold nanowires. Microsyst. Nanoeng. 4, 17084. https://doi.org/10.1038/micronano.2017.84.

Ivanova, N.V., Dewaard, J.R., Herbert, P.D.N., 2006. An inexpensive, automation-friendly protocol for recovering high-quality DNA. Mol. Ecol. Notes 6, 998–1002. https://doi.org/10.1111/j.1471-8286.2006.01428.x.

Kaarj, K., Akarapipad, P., Yoon, J.-Y., 2018. Simpler, faster, and sensitive zika virus assay using smartphone detection of loop-mediated isothermal amplification on paper microfluidic chips. Sci. Rep. 8, 12438. https://doi.org/10.1038/s41598-018-30797-9.

Kozel, T.R., Burnham-Marusich, A.R., 2017. Point-of-care testing for infectious diseases: past, present, and future. J. Clin. Microbiol. 55, 2313–2320. https://doi.org/10.1128/JCM.00476-17.

Kühnemund, M., Hernández-Neuta, I., Sharif, M.I., Cornaglia, M., Gijs, M.A.M., Nilsson, M., 2017. Sensitive and inexpensive digital DNA analysis by microfluidic enrichment of rolling circle amplified single-molecules. Nucleic Acids Res. 45, gkw1324. https://doi.org/10.1093/nar/gkw1324.

Liu, L., Guo, Z., Huang, Z., Zhuang, J., Yang, W., 2016. Size-selective separation of DNA fragments by using lysine-functionalized silica particles. Sci. Rep. 6, 22029. https://doi.org/10.1038/srep22029.

Mezger, A., Fock, J., Antunes, P., Østerberg, F.W., Boisen, A., Nilsson, M., Hansen, M.F., Ahlford, A., Donolato, M., 2015. Scalable DNA-based magnetic nanoparticle agglutination assay for bacterial detection in patient samples. ACS Nano 9, 7374–7382. https://doi.org/10.1021/acsnano.5b02379.

Mezger, A., Öhrmalm, C., Herthnek, D., Blomberg, J., Nilsson, M., 2014. Detection of rotavirus using padlock probes and rolling circle amplification. PLoS One 9. https://doi.org/10.1371/journal.pone.0111874.

Modak, S.S., Barber, C.A., Geva, E., Abrams, W.R., Malamud, D., Ongagna, Y.S.Y., 2016. Rapid point-of-care isothermal amplification assay for the detection of malaria without nucleic acid purification. Infect. Dis. 9, 1–9. https://doi.org/10.4137/IDRT.S32162.

Neumann, F., Hernández-Neuta, I., Grabbe, M., Madaboosi, N., Albert, J., Nilsson, M., 2018. Padlock probe assay for detection and subtyping of Seasonal influenza. Clin. Chem. 2018, 292979. https://doi.org/10.1373/clinchem.2018.292979.

Nilsson, M., Malmgren, H., Samiotaki, M., Kwiatkowski, M., Chowdhary, B.P., Landegren, U., 1994. Padlock probes: circularizing oligonucleotides for localized DNA detection. Science (80-.). https://doi.org/10.1126/science.7522346.

Obahiagbon, U., Smith, J.T., Zhu, M., Katchman, B.A., Arafa, H., Anderson, K.S., Blain Christen, J.M., 2018. A compact, low-cost, quantitative and multiplexed fluorescence detection platform for point-of-care applications. Biosens. Bioelectron. 117, 153–160. https://doi.org/10.1016/J.BIOS.2018.04.002.

Pimentel, A.C., Prazeres, D.M.F., Chu, V., Conde, J.P., 2008. Fluorescence detection of DNA using an amorphous silicon p-i-n photodiode. J. Appl. Phys. 104, 054913. https://doi.org/10.1063/1.2976343.

Pinto, I.F., Caneira, C.R.F., Soares, R.R.G., Madaboosi, N., Aires-Barros, M.R., Conde, J.P., Azevedo, A.M., Chu, V., 2017. The application of microbeads to microfluidic systems for enhanced detection and purification of biomolecules. Methods 116, 112–124. https://doi.org/10.1016/J.YMETH.2016.12.005.

Pinto, I.F., Santos, D.R., Caneira, C.R.F., Soares, R.R.G., Azevedo, A.M., Chu, V., Conde, J.P., 2018a. Optical biosensing in microfluidics using nanoporous microbeads and amorphous silicon thin-film photodiodes: quantitative analysis of molecular recognition and signal transduction. J. Micromech. Microeng. 28, 094004. https://doi.org/10.1088/1361-6439/aac66c.

Pinto, I.F., Santos, D.R., Soares, R.R.G., Aires-Barros, M.R., Chu, V., Azevedo, A.M., Conde, J.P., 2018b. A regenerable microfluidic device with integrated valves and thin-film photodiodes for rapid optimization of chromatography conditions. Sens. Actuators B Chem. 255, 3636–3646. https://doi.org/10.1016/J.SNB.2017.09.167.

Poeckh, T., Lopez, S., Fuller, A.O., Solomon, M.J., Larson, R.G., 2008a. Adsorption and elution characteristics of nucleic acids on silica surfaces and their use in designing a miniaturized purification unit. Anal. Biochem. 373, 253–262. https://doi.org/10.1016/j.ab.2007.10.026.

Poeckh, T., Lopez, S., Fuller, A.O., Solomon, M.J., Larson, R.G., 2008b. Adsorption and elution characteristics of nucleic acids on silica surfaces and their use in designing a miniaturized purification unit. Anal. Biochem. 373, 253–262. https://doi.org/10.1016/j.ab.2007.10.026.

Price, C.W., Leslie, D.C., Landers, J.P., 2009. Nucleic acid extraction techniques and application to the microchip. Lab Chip 9, 2484. https://doi.org/10.1039/b907652m.

Rodriguez, N.M., Linnes, J.C., Fan, A., Ellenson, C.K., Pollock, N.R., Klapperich, C.M., 2015. Paper-based RNA extraction, in situ isothermal amplification, and lateral flow detection for low-cost, rapid diagnosis of influenza A (H1N1) from clinical specimens. Anal. Chem. 87, 7872–7879. https://doi.org/10.1021/acs.analchem.5b01594.

Russell, C., Welch, K., Jarvius, J., Cai, Y., Brucas, R., Nikolajeff, F., Svedlindh, P., Nilsson, M., 2014. Gold nanowire based electrical DNA detection using rolling circle amplification. ACS Nano 8, 1147–1153. https://doi.org/10.1021/nn4058825.

Sanjuán, R., Nebot, M.R., Chirico, N., Mansky, L.M., Belshaw, R., 2010. Viral mutation rates. J. Virol. 84, 9733–9748. https://doi.org/10.1128/JVI.00694-10.

Santos, D.R., Soares, R.R.G., Chu, V., Conde, J.P., 2017. Performance of hydrogenated amorphous silicon thin film photosensors at ultra-low light levels: towards attomole sensitivities in labon- chip biosensing applications. IEEE Sens. J. https://doi.org/10.1109/JSEN.2017.2751253. (1–1).

Sato, K., Tachihara, A., Renberg, B., Mawatari, K., Sato, K., Tanaka, Y., Jarvius, J., Nilsson, M., Kitamori, T., 2010. Microbead-based rolling circle amplification in a microchip for sensitive DNA detection. Lab Chip 10, 1262–1266. https://doi.org/10.1039/b927460j.

Shi, B., Shin, Y.K., Hassanali, A.A., Singer, S.J., 2015. DNA binding to the silica surface. J. Phys. Chem. B 119, 11030–11040. https://doi.org/10.1021/acs.jpcb.5b01983.

Sin, M.L.Y., Mach, K.E., Wong, P.K., Liao, J.C., 2014. Advances and challenges in biosensor-based diagnosis of infectious diseases. Expert Rev. Mol. Diagn. 14, 225–244. https://doi.org/10.1586/14737159.2014.888313.

Soares, R.R.G., Santos, D.R., Pinto, I.F., Azevedo, A.M., Aires-Barros, M.R., Chu, V., Conde, J.P., 2018. Multiplexed microfluidic fluorescence immunoassay with photodiode array signal acquisition for sub-minute and point-of-need detection of mycotoxins. Lab Chip 18, 1569–1580. https://doi.org/10.1039/C8LC00259B.

Stumpf, F., Schwemmer, F., Hutzenlaub, T., Baumann, D., Strohmeier, O., Dingemanns, G., Simons, G., Sager, C., Plobner, L., von Stetten, F., Zengerle, R., Mark, D., 2016. LabDisk with complete reagent prestorage for sample-to-answer nucleic acid based detection of respiratory pathogens verified with influenza A H3N2 virus. Lab Chip 16, 199–207. https://doi.org/10.1039/C5LC00871A.

Taubenberger, J.K., Morens, D.M., 2008. The pathology of influenza virus infections. Annu. Rev. Pathol. 3, 499–522. https://doi.org/10.1146/annurev.pathmechdis.3.121806.154316.

WHO, 2018a. Influenza (Seasonal) [WWW Document]. URL 〈http://www.who.int/news-room/fact-sheets/detail/influenza-(seasonal). (Accessed 17 August 2018).

WHO, 2018b. Ebola virus disease [WWW Document]. URL 〈http://www.who.int/news-room/fact-sheets/detail/ebola-virus-disease. (Accessed 17 August 2018).

Wojciechowski, J.R., Shriver-Lake, L.C., Yamaguchi, M.Y., Fu¨reder, E., Pieler, R., Schamesberger, M., Winder, C., Prall, H.J., Sonnleitner, M., Ligler, F.S., 2009. Organic photodiodes for biosensor miniaturization. Anal. Chem. 81, 3455–3461. https://doi.org/10.1021/ac8027323.

Yoo, S.M., Lee, S.Y., 2016. Optical biosensors for the detection of pathogenic microorganisms. Trends Biotechnol. 34, 7–25. https://doi.org/10.1016/J.TIBTECH.2015.09.012.